PHYSICAL REVIEW B **71**, 104420 (2005)

Diffractive magneto-optics, magnetic interactions, and reversal mechanisms in Co microsquare arrays

J. L. Costa-Krämer,* R. Alvarez-Sánchez, A. Bengoechea, F. Torres, P. García-Mochales, and F. Briones
Instituto de Microelectrónica de Madrid, IMM (CNM-CSIC), Isaac Newton 8, PTM 28760, Tres Cantos, Spain
(Received 18 August 2004; revised manuscript received 9 December 2004; published 28 March 2005)

The magneto-optical properties of Co microsquare—2 μm edge—arrays have been investigated for different interelement separations, from 0.2 to 2.0 μm. The magneto-optical response is measured both at reflected and diffracted beams, and it is compared with the results of a model that uses micromagnetic simulations and optical diffraction theory to calculate the magneto-optical response for different diffracted spots. A satisfactory agreement between the experiments and the predictions from the combined micromagnetic and optical diffraction models allows the interpretation of the experimental data and provides a way to analyze and understand the physical meaning of the magneto-optic diffracted signal. The comparison of this diffracted magneto-optical experimental data with predictions from simple reversal models allows us to monitor different element magnetization reversal mechanisms as the separation between elements in the array varies.

DOI: 10.1103/PhysRevB.71.104420 PACS number(s): 75.75.+a, 75.60.Jk, 78.20.Ls

I. INTRODUCTION

Microstructured and, more recently, nanostructured samples have created much interest in recent years because of their potential applications in optical and magnetical storage devices. Particular attention has been given to the magnetical and magneto-optical properties of periodic arrays of micron and submicron elements of very different shapes, especially dots and stripes. The study of these arrays of submicron elements is the basis for the development of magnetic memories and nanopatterned recording media, as interelement interaction determines the integration limits of magnetic memories and nanopatterned recording media. The effect of the interaction between elements in the array has been much less studied than the effect of the size reduction. Magneto-optic techniques and, in particular, diffraction magneto-optic Kerr effect (DMOKE) are most suited to investigate experimentally such effects, since they show the high sensitivity needed to monitor magnetization changes in thin films and very small elements. We have previously shown also that DMOKE supplies valuable information also on the magnetization distribution[1] and anisotropy[2] due to its high sensitivity to magnetic inhomogeneities. This high sensitivity may provide the magnitude of the anisotropy constants, analyzing the array response on both the reflected and diffracted spots.[2] In the literature not only positive,[3] but negative arrays[4] have been studied using magneto-optic (MO) techniques. The importance of DMOKE is growing in recent years. This technique has been recently used to study patterned one-dimensional (1D)[5–7] and two-dimensional (2D)[7–10] thin films and also for negative magnetic arrays.[11–13] MO loops measured in different diffraction orders reveal marked differences with the loops measured at the reflected (zeroth order) beam. These differences are more marked as the elements are placed closer in the array, as will be shown below, and the question is: To what extent are these differences a signature of magnetic interactions between elements within the array?

A previous work[14] has revealed that the interaction threshold for 200-Å-thick Fe microelements is around 1 μm. This was deduced from the dependence of the saturation field on the separation between elements, decreasing as the distance is reduced. This is expected, since for an isolated element at magnetic saturation the demagnetization field is created by the surface poles. As another magnetic element is placed nearby some of the flux departs, decreasing the internal field and, consequently, the field required to saturate it. Since Co and Fe have very similar saturation magnetization values at room temperature (RT), and magnetic interactions are magnetostatic in origin, a similar value for Co micropatterned arrays is expected. The samples designed for this work consist of squares 2 μm of edge with separations in a range close to the assumed interacting range, 0.2, 0.5, 1.0, and 2.0 μm. These separations are available both for lithographic techniques and micromagnetic simulations.

In addition, micromagnetic modeling is not only highly valuable for interpreting and calculating magnetic interactions, but it permits us also to set the basis for an extended model in which electromagnetic fields interact with the array.[1,4,12] In this way, DMOKE effects can be modeled and interpreted using micromagnetic simulations combined with conventional optical diffraction theory.

II. EXPERIMENTAL SETUP

The magnetic properties of arrays of polycrystalline Co squares of 2 μm edge and 400 Å thickness are studied for arrays with elements of the same size and different interelement separation. The square arrays are fabricated in a 250 $\times$ 250 μm^2 field by conventional *e*-beam lithography on a continuous 400-Å-thick Co film. The film is deposited by triode sputtering at RT on a silicon substrate. The RT-triode-sputtered Co film exhibits a uniaxial anisotropy with an easy axis that is parallel to the plasma-confining field during deposition and an anisotropy field of 30 Oe. The magnetic properties of the thin film are totally consistent with a Stoner model, i.e., the hysteresis loop depends on the angle of the applied magnetic field with respect to the anisotropy axis, being square with a 30 Oe coercive field when the external

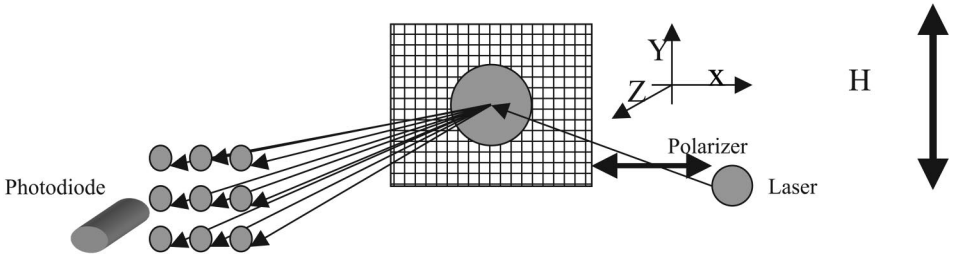

FIG. 1. Magneto-optic setup for tile array measurements.

field is applied along the easy magnetization axis and linear with a saturation field of 30 Oe when the external field is applied along the hard magnetization axis.

The film is patterned as follows: the deposited Co film is spin coated by a thin polymethylmethacrylate (PMMA) film, which is subsequently irradiated in a scanning electron microscope and developed. This PMMA layer is used as a mask in an ion beam etching procedure using Ar^+ ions. Typically we introduce about 25% overetching in order to ensure that the continuous film is properly patterned, i.e., the ion-milled trenches are deeper than the film.

The magnetic response of the arrays is measured by the transverse magneto-optic Kerr effect (MOKE) (Fig. 1), focusing a He-Ne laser ($\lambda = 630$ nm, 1.5 mW) within the array with an angle of incidence of 60°. A Helmholtz coil is used to generate a uniaxial magnetic field, *H*, parallel to one of the

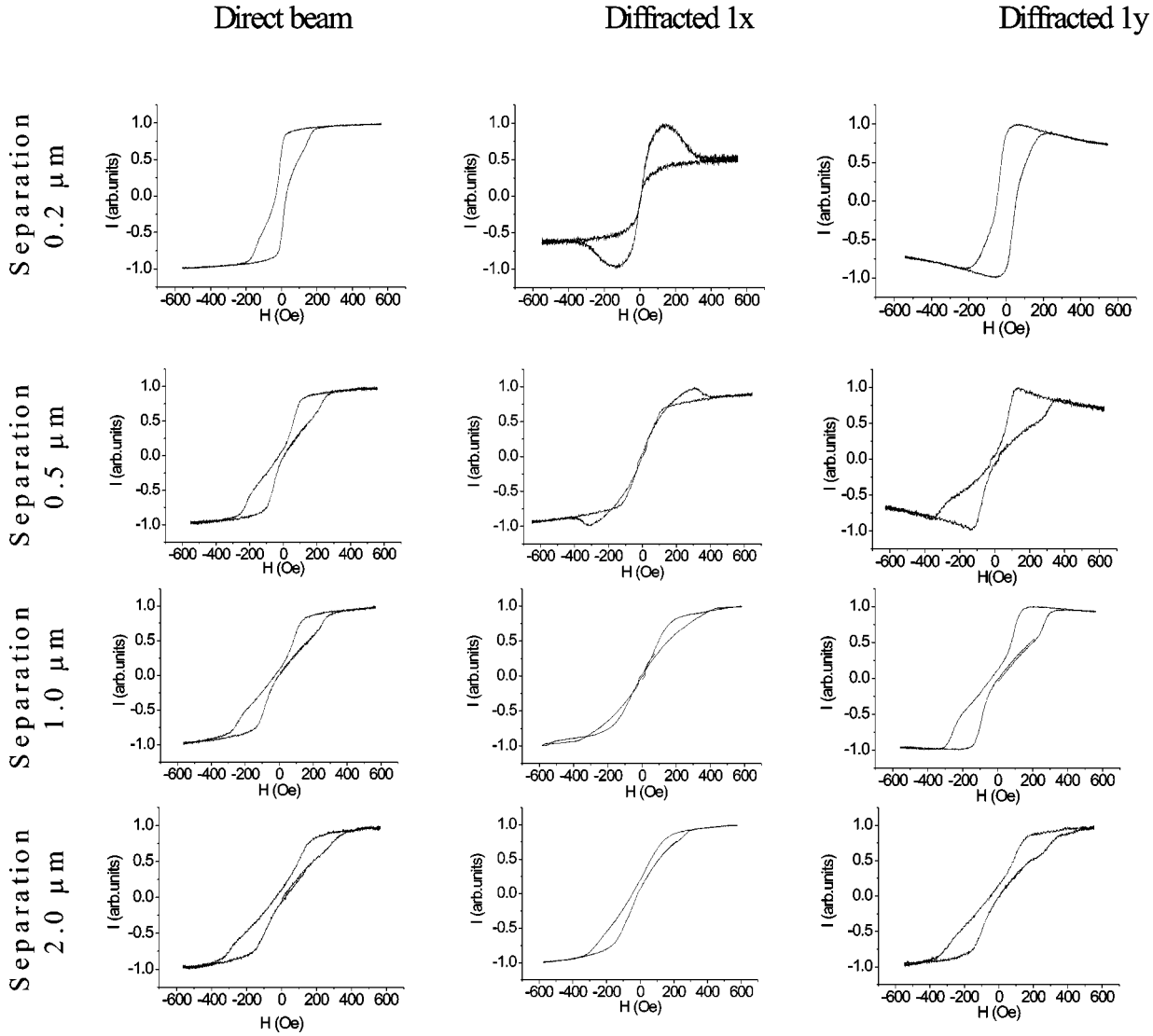

FIG. 2. Hysteresis loops, both for the zeroth order (reflected) and first *X* and *Y* diffracted orders, for arrays of 2 μm separated by 0.2 μm, 0.5 μm, 1.0 μm, and 2.0 μm with an external field *H* parallel to the Co uniaxial anisotropy easy axis.

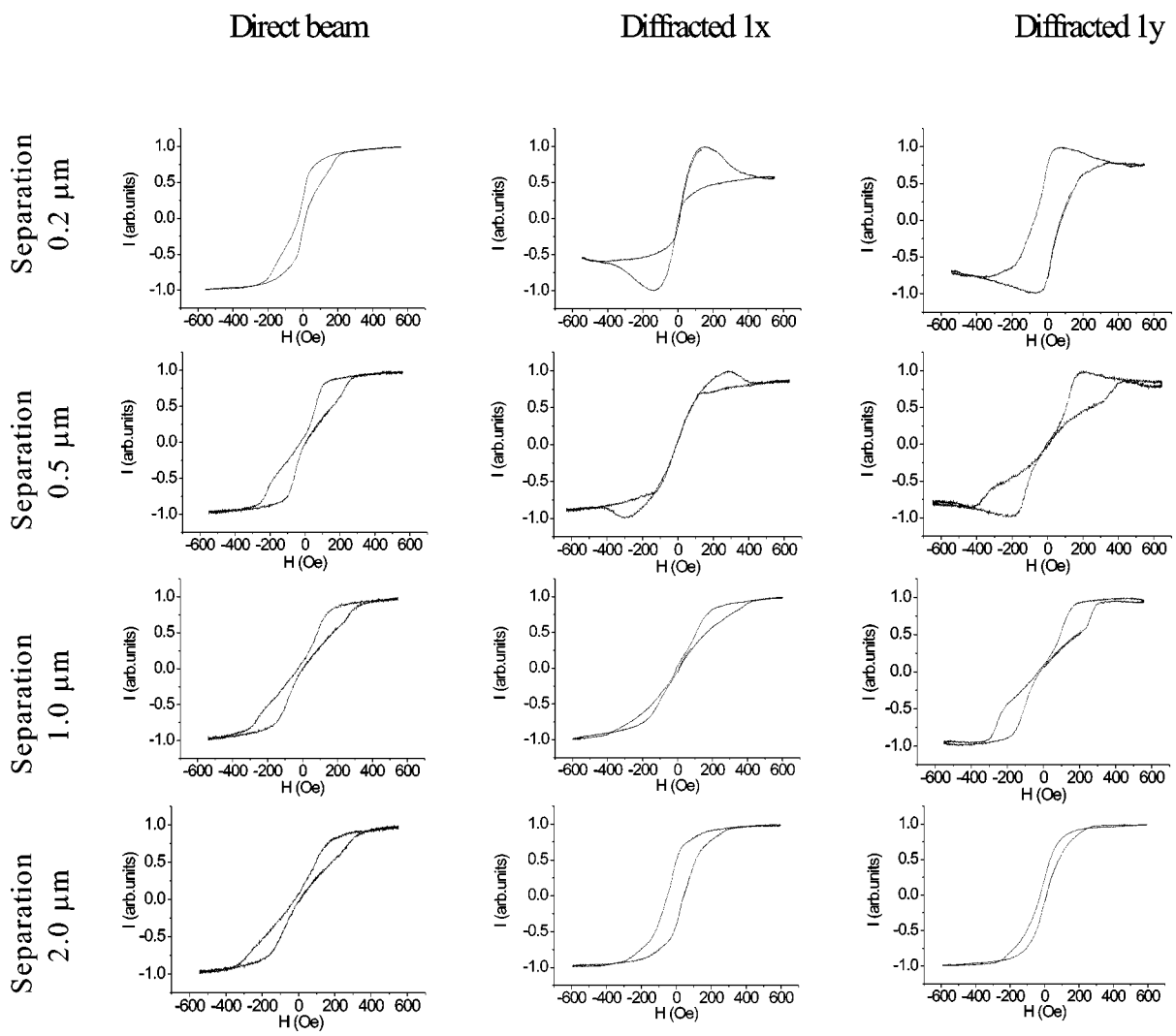

FIG. 3. Hysteresis loops, both for the zeroth order (reflected) and first X and Y diffracted orders, for arrays of 2 μm separated by 0.2 μm, 0.5 μm, 1.0 μm, and 2.0 μm with an external field H parallel to the Co uniaxial anisotropy hard axis.

square edges and perpendicular to the plane of incidence. The coil is fed with a sinusoidal current and provides 70 Oe per ampere circulating through the windings. The incident laser beam is p-polarized and after the reflection in the sample a diffraction pattern is obtained in which the p-polarized component can be measured for each diffraction spot using the photodiode. The Co anisotropy axis lies along the edge of the tiles.

III. RESULTS AND DISCUSSION

Upon illuminating the array in the Kerr setup, a diffracted pattern appears (see Fig. 1). Previous works have demonstrated that different diffracted orders (termed diffracted nX to the nth spot in the incidence plane and diffracted mY to the mth spot perpendicular to the incidence plane) provide different loops, markedly different from the loops obtained at the reflected zeroth order.[2,3,5,9] In this work we focus the analysis in the first order ($1X$ and $1Y$) magneto-optical dependencies, but a similar analysis can be easily performed for higher orders. The hysteresis loops obtained for the direct-reflected beam and for the first diffraction orders ($1X$ and $1Y$) when changing the intertile distance are shown in Fig. 2 (applying the external field parallel to the Co easy axis) and Fig. 3 (applying the external field parallel to the Co hard axis).

Comparing the measured hysteresis loops of Figs. 2 and 3, it is observed that there is no considerable effect on the MOKE signals of the direction of the Co anisotropy axis with respect to the applied field direction. This points to a magnetization process mainly dictated by the size of the elements and perhaps the interaction between them. This is expected, since demagnetizing fields (the loops saturate at about 400 Oe) are at least 1 order of magnitude larger than the Co anisotropy field, 30 Oe. In addition, there is no significant variation of the shape of the reflected beam (zeroth order) MO response when changing the intertile separation at constant tile size. However, there is a slight tilt of the loop that increases as the elements are separated further, in agreement with the previous consideration of a demagnetizing field of an isolated element that decreases as another element is placed closer and interaction starts.

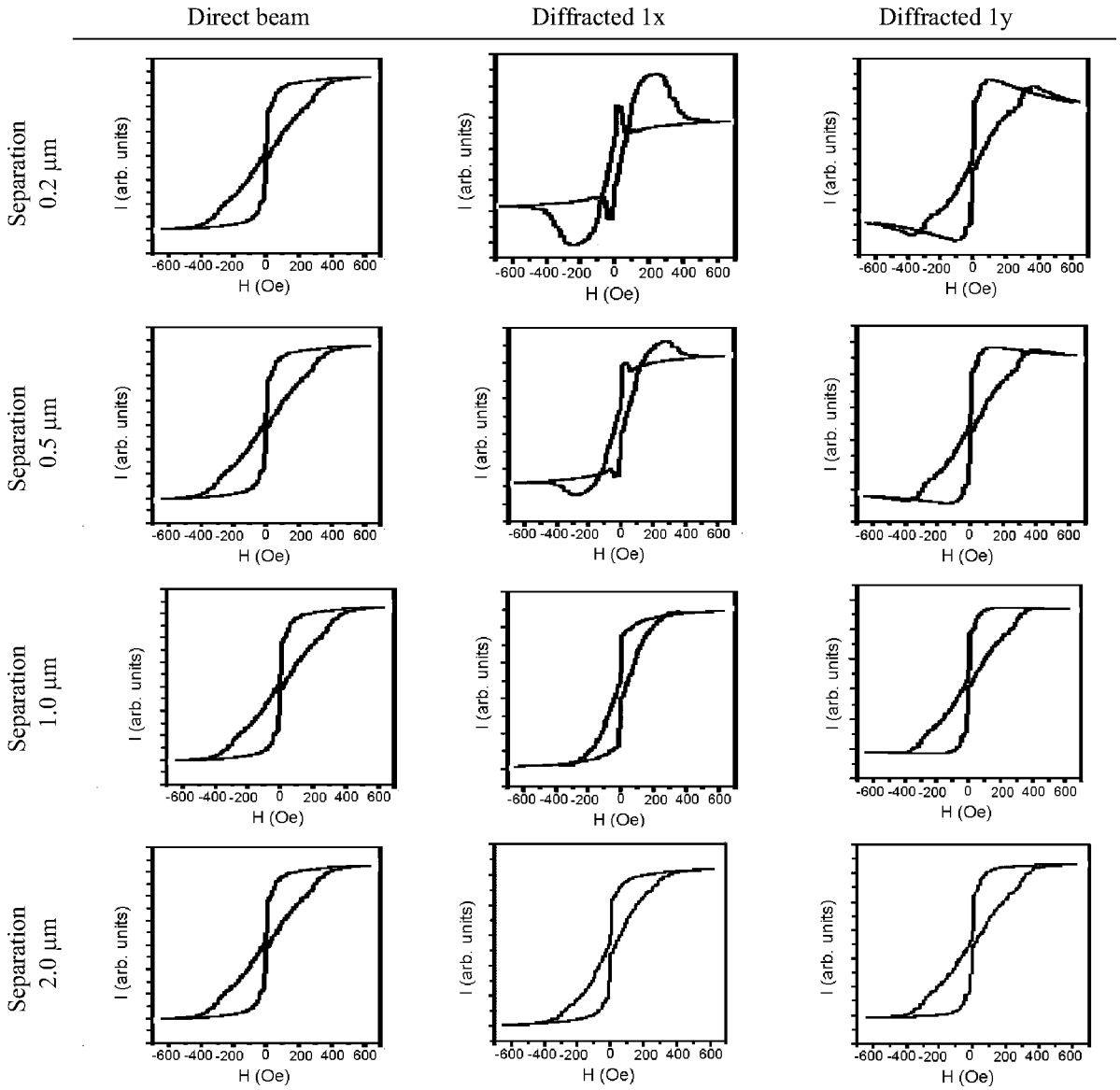

FIG. 4. Micromagnetic simulations and the expected MO dependencies in the first diffraction orders calculated using conventional optical diffraction theory for arrays of 2 μm separated by 0.2 μm, 0.5 μm, 1.0 μm, and 2.0 μm with H parallel to the Co uniaxial anisotropy easy axis.

Contrary to what is observed in the reflected spot magneto-optical component, the diffractive magneto-optical components change considerably when changing the inter-element separation. The DMOKE signals present some "anomalies" compared to conventional hysteresis loops. First, the reversibility branches of the loop happen, in general, at larger fields than in the reflected loop. The 1X MO loops display a region where the MO signal is larger than at saturation, decreasing as the distance between elements is increased. The 1Y MO loops display a negative slope at the reversibility branch, close to saturation, that again decreases as the distance between elements is increased.

All these experimental results can be correlated with micromagnetic simulations (OOMMF public code v. 1.1b @ http://math.nist.gov/oommf/). The OOMMF code solves the magnetic part of the problem providing a distribution for the magnetization for an isolated square element for each field value. Measuring our samples using the transverse Kerr effect means that the reflectivity is proportional to the magnetization component along the field direction, without higher order contributions. This way, the M_y component of the magnetization provided by the simulation, which corresponds to the transversal Kerr effect signal, provides a reflectivity distribution. Then, assuming identical reflectivity distributions for every element, a diffraction pattern can be calculated using conventional optical diffraction theory, and once the positions of the diffracted maxima are determined, the expected MO intensity evolution as a function of the external applied magnetic field can be calculated (Fig. 4).

Our aim is then to develop the simplest model that describes diffractive magneto-optical signals in magnetic arrays. To do so, the problem is separated into two: (1) to obtain reasonable magnetization distributions as a function of the external field and then (2) to use these distributions to

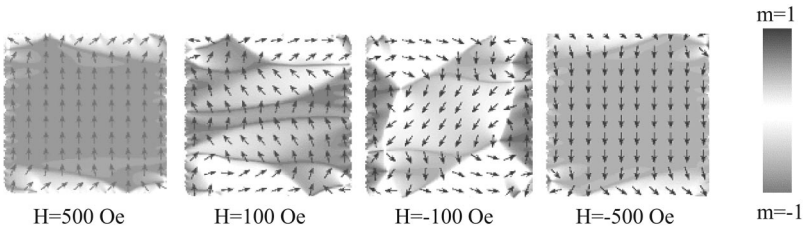

FIG. 5. Magnetization distribution in a single square element of the array for different values of the external field H. Only m_y, which corresponds to the transversal Kerr effect signal, is displayed in color code.

calculate the expected diffracted magneto-optical signals.

As no significant differences are observed between applying the field along the Co easy or hard axis, the comparison between the experimental data and the micromagnetic simulations will be presented just for the easy axis case. The simulated hysteresis loops for different interelement distances for both the reflected and first diffraction orders are shown in Fig. 4.

For simplicity and computational time optimization these micromagnetic simulations have been performed assuming that the array is composed of noninteracting tiles. Thus, all direct-beam hysteresis loops are equal regardless of their separations. Then, the slight difference between experiments and simulation in the direct-beam hysteresis loops has to be attributed to interaction effects. As observed, there are great similarities between the experiments (Fig. 2) and the simulations (Fig. 4) that can serve to describe the magnetization processes. It has been already mentioned that in the transversal Kerr configuration the measured reflectivity is proportional to the magnetization component parallel to the applied field, without higher order contributions. As such, the measured direct-beam MO response represents the array's average magnetization and its corresponding hysteresis loops show the evolution of the average magnetization per element when changing the applied external field.

Hysteresis loops for different intertile distances show the same shape: a zero-field area close to reversibility linking two loops. As shown by the micromagnetic simulations (see Fig. 5) this behavior is due to a two-phase magnetization inversion: first the center stripe and then the edges parallel to the field direction.

Although all the direct-beam hysteresis loops exhibit the same shape, an increase in the separation between elements

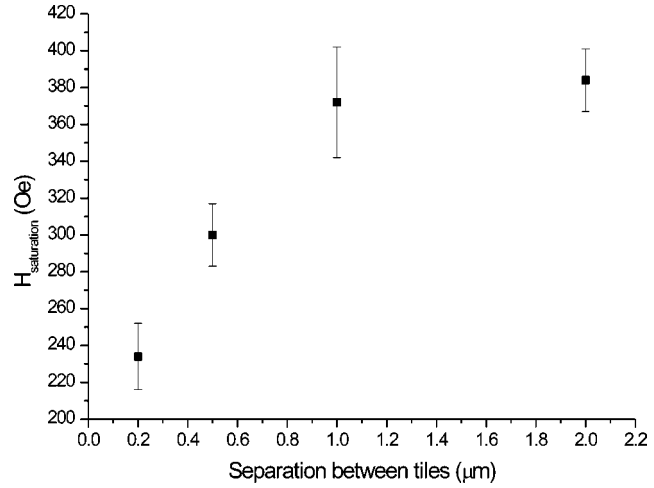

FIG. 6. Saturation field vs intertile distance.

implies an increase in the saturation field, i.e., an increase in the value of the external field needed to reach saturation (see Fig. 6).

The applied field is not the effective field acting on the different elements due to a demagnetizing field that opposes the applied field. The effective (or internal) field on an element is the difference between the applied field and the demagnetizing field ($H_{\text{eff}}=H_{\text{applied}}-H_{\text{demag}}$). The sudden drop of the saturation field when reducing the separation between elements means that the internal field increases as the distance between elements decreases. Accordingly the demagnetizing field H_{demag} decreases when the separation decreases. This suggests that at low separations, indicating the onset of the interaction, part of the magnetic flux closes between different tiles, i.e., tiles are interacting. Then Fig. 6 implies interaction between tiles when their separation is below 1 μm, similar to what is observed for Fe epitaxial tilings of similar dimensions.[14]

So far, it has been shown that the average magnetization (as seen by the zeroth order MO loop) measured in the arrays is described reasonably well by an ensemble of noninteracting elements with the same magnetization distribution, and the effect of the distance between elements is to decrease the field necessary to saturate the array, symptomatic of an onset of the interactions. We proceed to describe the information accessible from the DMOKE loops. The MO contribution to the (n,m) diffracted spot follows:[1]

$$\text{Kerr\_signal}(n,m) \propto \text{Re}\left(B\int_{-a/2}^{a/2}\int_{-a/2}^{a/2} m_y(x,y)e^{2\pi inx/T}e^{2\pi imy/T}dxdy\right),$$

where $m_y(x,y)$ is the magnetization projection along the Y direction (which corresponds to the transversal MOKE signal), n and m are the X and Y diffraction orders respectively, a is the square length, T the period of the array ($T=a+w$, the square length a plus the intertile distance w), and B is a complex parameter that depends on the material, light wavelength, and incidence angle.[1,8,12] A similar theoretical formalism that accounts for the expected MO dependencies in diffracted MOKE signals is detailed in Ref. 15.

Differences in DMOKE signals can be explained as the effect of matching between the magnetization distribution and the moment associated to the periodicity of the array (Fig. 7). The square arrays have been fabricated over a nonmagnetic substrate. This implies that $m_y(x,y)=0$ outside the square element, so the integration period is the square length. For the first diffraction orders ($n=1$, $m=0$ for diffracted $1X$ and $n=0$, $m=1$ for diffracted $1Y$) the magnetization is weighted by a factor, either $\cos(2\pi x/T)$ or $\cos(2\pi y/T)$, that

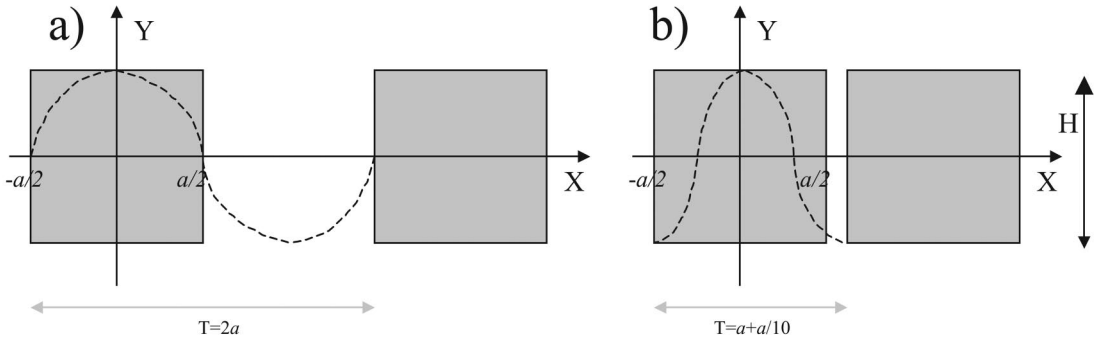

FIG. 7. Matching of the weighting factor for the diffracted 1*X* signal for (a) *a* and (b) $a/10$ intertile distances.

directly depends on the array motif period *T*. As $T=a+w$, different separations imply different weightings of the magnetization distribution, so different diffracted hysteresis loops are expected just because of the geometry of the array.

As shown in Fig. 7(a), when the array period *T* is twice the length of the tile (corresponding to 2 μm intertile distance for 2 μm edge elements), the weighting function is positive all over the tile, so the corresponding diffracted 1*X* hysteresis loop should be similar to the direct beam one, as it occurs for this case (Fig. 2, 2 μm separation). On the other hand, when the motif period *T* approaches the length of the tile (which corresponds to the continuum), the weighting factor is positive at the center of the tile and negative at the edges parallel to the field direction. Then, the magnetization at the edges that runs parallel to the field direction weights more, and negatively, for smaller interelement distances [Fig. 7(b)]. The Kerr formula for the diffracted intensities tells us that, depending on the interelement separation, there are magnetization distributions [for instance, an $M_y(x)$ where the central part of the element has switched and the magnetization close to the edges has not switched yet] that have a higher moment than in the saturated state. This explains the anomalous "bump" in the first *X* diffracted loop where the signal is larger than at magnetic saturation (Fig. 2, 0.2 μm

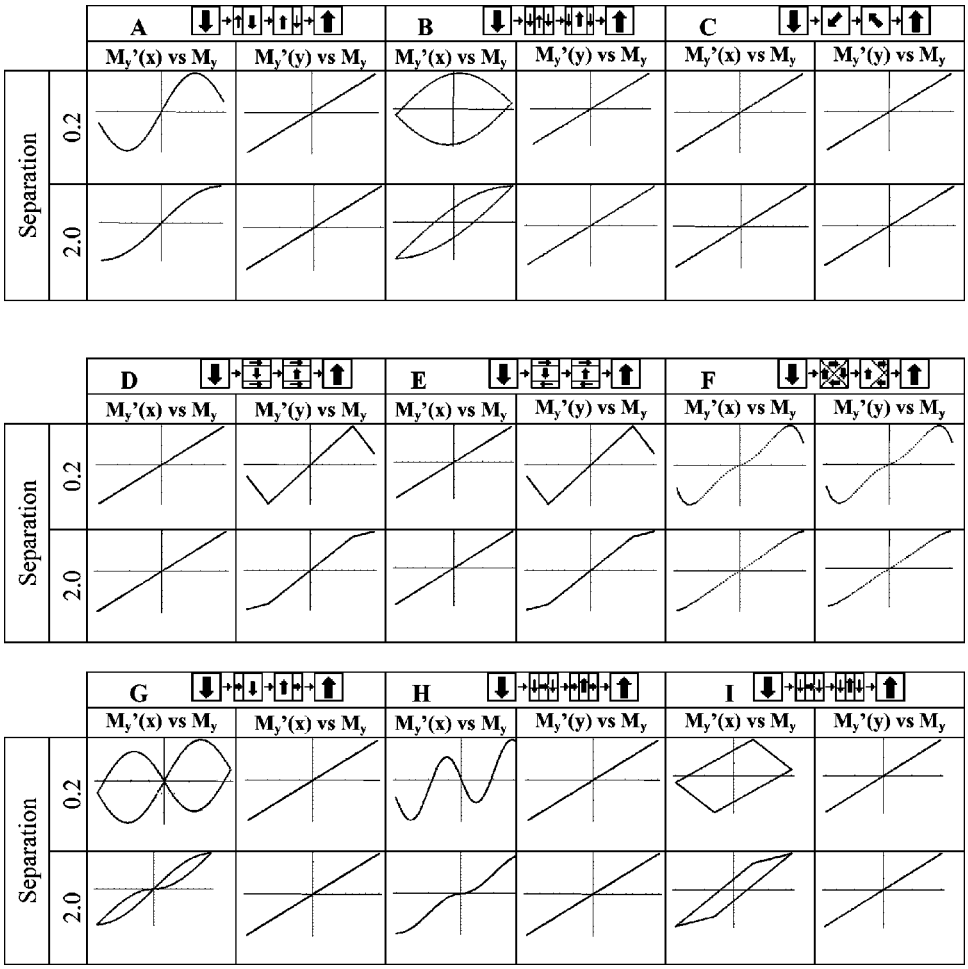

FIG. 8. Diffracted signals 1*X* and 1*Y* vs magnetization for different inversion processes: (a) propagation of a single 180° domain wall parallel to the applied field, (b) propagation of two 180° domain walls parallel to the applied field, (c) coherent rotation of the magnetization, (d) *S* state with domain walls situated at 1/6 square length of the edge, (e) *C* state with domain walls situated at 1/6 square length of the edge, (f) vortex displacement along the *X* axis, (g) two consecutive propagations of a single 90° domain wall, (h) two consecutive propagations of two simultaneous 90° domain walls, (i) rotation at the center of the element is followed by a rotation at the borders.

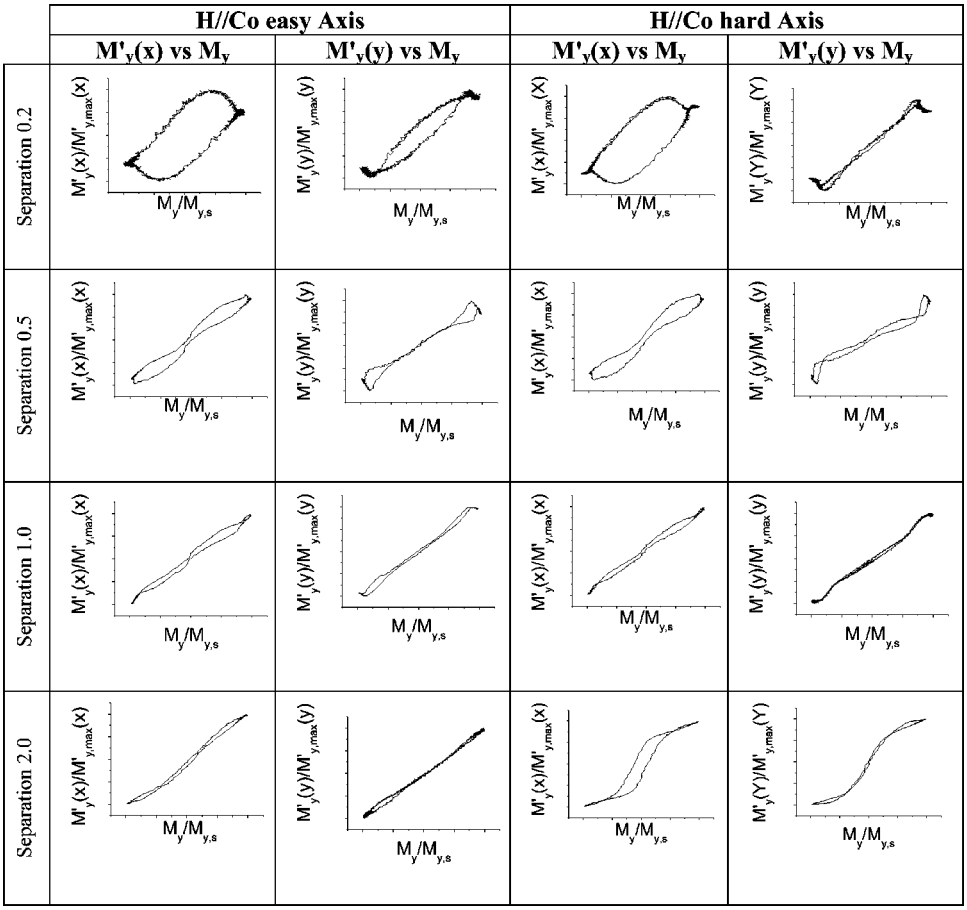

FIG. 9. Experimental first order diffracted MO signal vs average magnetization for different interelement (from 0.2 to 2 μm) separations. Data are shown when the field is applied both along the easy and the hard Co axes and parallel to the 2 μm Co square element.

separation). Similar arguments can be applied to $M_y(y)$ and the first Y diffraction order. This matching effect is crucial to understanding the observed MO dependencies in the diffracted spots and renders this technique quite useful to discern different reversal mechanisms, as shown below.

This way, both the apparent higher saturation field in the $1X$ and $1Y$ DMOKE loops and the anomalous bumps and slopes are explained. Although the element has almost reached magnetic saturation, the DMOKE signal is much more sensitive to the magnetization at the edges for closer interelement separations. Summarizing, the nth DMOKE loop represents the nth Fourier moment of the magnetization distribution. In particular, diffracted $1X$ ($1Y$) represents the first Fourier moment of the magnetization distribution projection on the X (Y) axis averaged in the Y (X) axis, $M_y'(x)$ $[M_y'(y)]$. In spite of the high sensitivity of the DMOKE signal to the interelement separation, there is no obvious signature of the onset of the interaction between elements that can be obtained from the DMOKE signals, as their high sensitivity is due to the matching of the array periodicity and the weighting factor. However, this DMOKE signal, being an average information of all the array elements, contains information about the magnetization distributions during reversal, which in the case of interacting elements might be different from those for isolated elements, due to the different local field distributions associated.

The DMOKE signal is then highly correlated with the magnetization distribution and the periodicity of the array. If we graph one of the magnetization distribution moments as a function of the average magnetization (zeroth moment), we find that different reversal mechanisms produce distinct dependencies. Thus, one convenient way to analyze and compare data for different reversal models is to plot each diffracted signal as a function of the reflected signal which is proportional to the average magnetization. This allows us to analyze different magnetization reversal processes, irrespective of the applied field necessary to produce them. This way our experimental data can be correlated with very simple (because the field is not required here either) reversal simulations. Different diffracted signals vs average magnetization plots can be obtained for different magnetization distributions. Some illustrative examples are shown in Fig. 8.

Reversals driven by coherent rotations produce linear reversible dependencies of the diffracted signals X and Y on the average magnetization. Domain walls parallel (perpendicular) to the applied field direction that produce sinusoidal dependencies of the X (Y) component and linear dependencies of the Y (X). The C and S states show a linear X component and a continuous, piecewise-defined Y component. Finally, a vortexlike state presents pseudosinusoidal dependencies in both X and Y components. The plots shown in Fig. 8 can be compared with the experimental data in Fig. 9 that shows the experimental diffracted signals vs average magnetization for different separations obtained from the data shown in Figs. 2 and 3. As expected, the data shown in Fig. 9 present again a minor relevance of the direction of the field with respect to the Co easy axis, as discussed in Figs. 2 and 3, due to demagnetizing fields (loops saturate at about

400 Oe) at least one order of magnitude larger than the Co anisotropy field.

The results obtained from the combined micromagnetic simulation and optical diffraction theories (see Fig. 4) are similar to the experimental ones shown in Fig. 9 and are not shown.

Although there is no clear correlation between the experiments shown and the predictions from the simple reversal models shown in Fig. 8 a few general conclusions can be made. The comparison between the simple reversal models and the obtained experimental data of the first order diffractive signals vs the average magnetization points to a reversal that for large interelement separations (2 μm) is a mixture of vortex [see Fig. 8(f)] and *C* or *S* states [Figs. 8(d) and 8(e)], while for small interelement distances (0.2 μm) the reversal is driven by the switching, first of the central stripe of the square, and then of the areas close to the edges. For intermediate separations (1 and 0.5 μm) the experimental data seem to adjust better to a combination of one 90° domain wall propagation [see Fig. 8(g)] and *C* or *S* states [Figs. 8(d) and 8(e)]. In this way, there would be a transition from flux closure within elements at large interelement distances, to flux closure between different elements at small interelement distances. Although quite qualitative, and using only the first diffraction order, the above discussion illustrates the power of using the DMOKE signal, i.e., using the different moments of the magnetization distribution to elucidate reversal mechanisms in magnetic arrays.

IV. SUMMARY

The MO properties of Co microsquare—2 μm edge, 40 nm thickness—arrays have been investigated for different interelement separations, from 0.2 to 2.0 μm, close to the magnetic interaction threshold of the order of 1 μm. There is no significant effect on the MOKE signals of the direction of the Co anisotropy axis with respect to the applied field direction, i.e., the magnetization processes are mainly dictated by the shape of the elements and perhaps by the interaction between them, i.e., the magnetostatics. The magneto-optical response is measured both at reflected and diffracted beams and compared with the results of a model that uses micromagnetic simulations and optical diffraction theory to calculate the magneto-optical responses for different diffracted spots. A satisfactory agreement between the experiments and the predictions from the combined micromagnetic and optical diffraction models allows for the interpretation of the experimental data and provides a way to analyze and understand the physical meaning of the magneto-optic diffracted signal. This is performed for the first order diffraction spots as an illustration. The anomalous loops observed in the DMOKE are not related in a clear manner to the onset of the interactions, but to the different matchings of the moment of the magnetization distributions to the periodicity of the array. The comparison of this diffracted magneto-optical experimental data with predictions from simple reversal models allows the characterization of different element magnetization reversal mechanisms as the separation between elements in the array varies.

ACKNOWLEDGMENT

R.A.S. acknowledges support from the "Consejería de Educación de la Comunidad de Madrid." Research funded through EC-G5RD-CT-2002–00731 HIDEMAR project.

*Email address: Kramer@imm.cnm.csic.es

[1] P. García-Mochales, J. L. Costa-Krämer, G. Armelles, F. Briones, D. Jaque, J. I. Martín, and J. L. Vicent, Appl. Phys. Lett. **81**, 3206 (2002).

[2] D. Jaque, J. I. Martín, G. Armelles, J. L. Costa-Krämer, F. Briones, and J. L. Vicent, J. Appl. Phys. **91**, 382 (2002).

[3] P. Vavassori, M. Grimsditch, V. Novosad, V. Metlushko, and B. Ilic, Phys. Rev. B **67**, 134429 (2003).

[4] I. Guedes, M. Grimsditch, V. Metlushko, P. Vavassori, R. Camley, B. Ilic, P. Neuzil, and R. Kumar, Phys. Rev. B **67**, 024428 (2003).

[5] T. Schmitte, T. Schemberg, K. Westerholt, and H. Zabel, J. Appl. Phys. **87**, 5630 (2000).

[6] Y. Souche, O. Geoffroy, V. Novosad, V. Pishko, and B. Pannetier, J. Magn. Soc. Jpn. **20-Sup S1**, 393 (1996).

[7] T. Schmitte, K. Westerholt, and H. Zabel, J. Appl. Phys. **92**, 4524 (2002).

[8] M. Grimsditch, P. Vavassori, V. Novosad, V. Metlushko, H. Shima, Y. Otani, and K. Fukamichi, Phys. Rev. B **65**, 172419 (2002).

[9] O. Geoffroy, D. Givord, Y. Otani, B. Pannetier, A. D. Santos, M. Schlenker, and Y. Souche, J. Magn. Magn. Mater. **121**, 516 (1993).

[10] P. Vavassori, V. Metlushko, M. Grimsditch, B. Ilic, P. Neuzil, and R. Kumar, Phys. Rev. B **61**, 5895 (2000).

[11] I. Guedes, N. J. Zaluzec, M. Grimsditch, V. Metlushko, P. Vavassori, B. Ilic, P. Neuzil, and R. Kumar, Phys. Rev. B **62**, 11 719 (2000).

[12] I. Guedes, M. Grimsditch, V. Metlushko, P. Vavassori, R. Camley, B. Ilic, P. Neuzil, and R. Kumar, Phys. Rev. B **66**, 014434 (2002).

[13] P. Vavassori, V. Metlushko, R. M. Osgood III, M. Grimsditch, U. Welp, and G. Crabtree, Phys. Rev. B **59**, 6337 (1999).

[14] J. L. Costa-Krämer, J. I. Martín, J. L. Menéndez, A. Cebollada, J. V. Anguita, F. Briones, and J. L. Vicent, Appl. Phys. Lett. **76**, 3091 (2000).

[15] M. Grimsditch and P. Vavassori, J. Phys.: Condens. Matter **16**, R275 (2004).